Simulating Adiabatic Parcel Rise

Anna Merrifield, Sarah Shackleton, and Jeff Sussman*
Scripps Institution of Oceanography, Department of Climate Science
(Dated: December 5, 2013)

Using simplified adiabatic parcel theory, we attempt to reproduce parcel behavior provided in Curry and Webster's Figure 7.2 with and without entrainment of dry air. From first principles, we derive lapse rates for dry adiabatic (Γ_d), saturated adiabatic (Γ_s), and saturated adiabatic entraining dry air (Γ_m) rise. Our study demonstrates that the provided parcel is not governed by simplified adiabatic parcel theory, but can be reproduced by back-engineering parcel lapse rates.

I. INTRODUCTION

The process of air parcel rise causes cloud formation and thunderstorm growth. Of the processes involved in cloud formation, the adiabatic cooling of moist air is one of the most important. A parcel of air, heated at the Earths surface, will begin to rise if it becomes warmer than its surroundings. The force on the parcel by the environment, called the buoyancy force, is positive and pushes the parcel upward. The magnitude of this upward motion is determined by the parcel's CAPE or *convective available potential energy*, defined as the "amount of energy available for upward acceleration" [2]. Determining CAPE in a parcel-environment system is crucial to understanding the atmospheric dynamics, but also in predicting events such as tornadoes and hurricanes. The better the accuracy of available models, the more we may predict these potentially detrimental weather events.

Modeling air parcel motion is often difficult, due to the many degrees of freedom of the system. One factor that affects parcel buoyancy in nature is entrainment, the incorporation of environmental air into a parcel. The magnitude of entrainment is an important factor in determining the buoyancy force. In our system, we show that a cloud entraining dry air from the environment will experience a reduction in CAPE, hindering its ability to rise. In nature, the entrainment of dry air in the mid levels of a thunderstorm will similarly reduce the buoyancy of the parcel and the amount of CAPE. Entrainment of dry air aloft in a thunderstorm, though, will intensify the negative buoyancy for a parcel in a downdraft, and increase the velocity of the downdraft.

II. THEORY AND METHODS

In this study of adiabatic parcel rise, we attempt to reproduce Figure 7.2 in Curry and Webster by constructing temperature profiles and plotting them on an aerological diagram against ln-scaled pressure, which approximately corresponds to height z. We consider two systems, first assuming the parcel, which henceforth has properties indicated with a prime, does not entrain environmental air. We then assume the entrainment of dry air into the saturated parcel. Each scenario is compared to a provided parcel and its accompanying environmental sounding (observed vertical property distribution, in this case temperature and pressure) to determine if it is possible to reproduce a physical phenomena using the simplified governing equations of adiabatic parcel theory.

The temperature profiles of a conditionally unstable air parcel and its environmental sounding provided in Figure 7.2 are plotted in Figure 1. "Conditionally unstable" means that an unsaturated air parcel is "stable to vertical displacement" ($\Gamma_d > \Gamma_{env}$) and does not rise, while a saturated parcel will rise if perturbed ($\Gamma_s < \Gamma_{env}$) [2]. The air parcel and environmental sounding begin at the same temperature at a pressure of 1000 hPa and approximately sea level. As height above the surfaces increases, atmospheric pressure falls, and from 1000 to 900 hPa, the unsaturated air parcel adiabatically expands and decreases in temperature. When the temperature of the parcel is less than that of the environment, the environment exerts a restoring force downwards on the parcel known as a negative buoyancy force, causing the parcel to oscillate stably about its initial state.

As the temperature decreases, the saturation vapor pressure of the parcel (e'_s) decreases, while the composition or mixing ratio (w'_s) of the parcel remains fixed (assuming no entrainment). The relative humidity (H') of the parcel thus increases. At 900 hPa, the air parcel reaches 100% relative humidity ($H' = 1$), which is known as the *lifting condensation level* (LCL), and becomes fully saturated. As the saturated parcel continues to rise, it follows a saturated adiabatic lapse rate. Air parcel and environment temperatures converge at 810 hPa, which is the *level of free convection* (LFC) at which the parcel experiences the necessary impulse to begin its convective ascent. From 810 to 530 hPa the temperature of the parcel is greater than that of the environment giving the parcel an upwards buoyancy force. At 530 hPa, the temperatures of the parcel and its surrounding environment again converge at the *level of neutral buoyancy* (LNB) above which the temperature of the environment exceeds that of the parcel, leading to a downward stabilizing force on the parcel.

Our first model run attempts to mimic the provided air parcel behavior without entrainment with the following simplifying assumptions: [2].

* almerrif@ucsd.edu, sshackle@ucsd.edu, jsussman@ucsd.edu

1. The parcel retains its identity and does not mix with its environment.

2. The parcel motion does not disturb the environment.

3. The pressure of a parcel adjusts instantaneously to that of its surrounding environment.

4. The parcel moves isentropically.

As temperature in the atmosphere varies with height i.e. $\frac{-dT}{dz} = \Gamma$, we first assumed a constant lapse rate environment over 3 intervals (Figure 2) and performed least-squares fits on the $\ln(P)\cdot\frac{R_d\bar{T}}{g}$ vs. T environmental sounding to gain approximate values of Γ_{env}. These values of Γ_{env} were used to find height Z according to

$$Z = \frac{To}{\Gamma_{env}} \cdot \left(1 - \left(\frac{P}{Po}\right)^{\frac{R_d\Gamma_{env}}{g}}\right) \tag{1}$$

where T_o and P_o are initial environmental values of temperature and pressure, respectively. Temperature profiles could then be calculated from the recursive relation:

$$T'_{k+1} = T'_k + \frac{dT'}{dz}|_k \cdot (Z_{k+1} - Z_k) \tag{2}$$

with $\frac{dT'}{dz} = -\Gamma$. Below the LCL, our model assumes the constant dry lapse rate of an ideal gas: $\Gamma_d = \frac{g}{c_{pd}}$. From the LCL to LNB, the air parcel is assumed to be at saturation, with no loss of water through precipitation. The saturated lapse rate, Γ_s, was derived from the combined first and second laws of an air parcel with moist air and a liquid water phase component. Assuming only liquid and vapor phases and a closed system and solving for $\mathrm{d}\eta$, we can write (3) as (4) Where w_t is total mixing ratio ($w_v + w_l$) and A_{lv} is the affinity for vaporization and is equal to $\mu_l - \mu_v$.

$$Td\eta = dH - VdP - \sum_j \mu_j dn_j \tag{3}$$

$$\begin{aligned} d\eta = (c_{pd} + w_t c_l)d(\ln T) - R_d d(\ln P_d) \\ + d(\frac{L_{lv}w_v}{T}) + w_v d(\frac{A_{lv}}{T}) \end{aligned} \tag{4}$$

To simplify, our model assumes that the system is at chemical equilibrium so that $A_{lv}= 0$, and a constant L_{lv}. The heat capacities of water vapor and liquid water are minimal, so these terms are neglected[2] and (4) is simplified to (5)

$$d\eta = c_{pd}d(\ln T) - R_d d(\ln P) + \frac{L_{lv}}{T}d(w_s) \tag{5}$$

$$\frac{dP}{P} = \frac{-g}{R_d T}dz \tag{6}$$

$$\frac{dw_s}{w_s} = \frac{de_s}{e_s} - \frac{dP}{P} \tag{7}$$

Because we assume our air parcel to be lifted adiabatically and reversibly, entropy is constant ($\mathrm{d}\eta = 0$). Incorporating the hypsometric equation (6) and the saturation mixing ratio (7), we can write (5) as (8). Dividing by increments of dz, applying the chain rule, and solving for $\frac{-dT}{dz}$ gets (9). Applying Clausius-Clapeyron and our dry air lapse rate (Γ_d), we finally obtain our models saturated lapse rate for an air parcel (10). Figure 3 compares the simulated parcel to the parcel provided. Above the LNB, the parcel is "moist" ($0 < H < 1$) and for our purposes can be assumed to follow a dry adiabat. By inspection of the calculated parcel to parcel provided, it was also clear Γ_d was too large for this region causing the simulated temperature profile to be too flat. A suitable value of Γ for this region, which matched the parcel provided, turned out to approximately be $3\frac{K}{Km}$ or about $\frac{\Gamma_d}{3}$. The physical interpretation of this value is forthcoming.

$$-L_{lv}w_s\left(\frac{de_s}{e_s} - \frac{dP}{P}\right) = c_p dT + gdz \tag{8}$$

$$\frac{-dT}{dz}\left(1 + \frac{L_{lv}w_s}{c_p e_s}\frac{de_s}{dT}\right) = \frac{g}{c_{pd}}\left(\frac{L_{lv}w_s}{R_d T} + 1\right) \tag{9}$$

$$\Gamma_s = \Gamma_d\left(\frac{1 + \frac{L_{lv}w'_s}{R_d T'}}{1 + \frac{\epsilon L_{lv}^2 w'_s}{c_{pd}R_d T'^2}}\right) \tag{10}$$

Our second model run includes the entrainment of dry air ($w_v = 0$) using a range of entrainment rates ($\lambda = \frac{1}{m}\frac{dm}{dz}$) between $5\cdot10^{-10}$ to $5\cdot10^{-4}$ $\frac{1}{m}$, consistent with ranges found in other independent studies [4][5] . The saturated entraining lapse rate, Γ_m was derived by applying the first law of thermodynamics to an open system ($m + dm$) to obtain the heat balance (11). Simplifying assumptions include:

1. No water precipitates out of the parcel

2. The heat transfers considered are changes in latent heat and specific heats of the system caused by the entrainment of dry air

3. The model assumes that entrainment rates remain constant with increasing height.

From (11) we can derive an equation for a lapse rate that includes the entrainment of dry air (12) Figures 4 shows temperature profiles for simulated parcels entraining $5\cdot10^{-10}$, $5\cdot10^{-5}$, $1\cdot10^{-4}$, and $5\cdot10^{-4}$ $\frac{1}{m}$.

$$\begin{aligned} m\left(c_{pd}dT' - R_d T'\frac{dP}{P}\right) \\ = -mL_{lv}dq_s - c_{pd}(T' - T)dm - L_{lv}(q'_s - q_v)dm \end{aligned} \tag{11}$$

$$\Gamma_m = \Gamma_s + \frac{\frac{1}{m}\frac{dm}{dz}\left((T' - T) + \frac{L_{lv}}{c_{pd}}(q'_s - q_v)\right)}{\left(1 + (\epsilon\frac{L_{lv}^2 q_s}{c_{pd}R_d T^2})\right)} \quad (12)$$

III. DISCUSSION

From sea level to the LCL, both of our model runs follow a dry adiabat, and reproduce the provided air parcel quite well. However, after the LCL, the model shows that the provided parcel cannot be reproduced from the simplified governing equations. Using the parameters detailed in Curry and Webster and assuming no entrainment, calculations of air parcel and atmospheric temperature versus pressure (Figure 2), show that air parcel temperature at any given height is less than that of the environment. This indicates the buoyant force on the parcel should always be in the downward direction, rendering the parcel absolutely stable. With entrainment of dry air, the Γ value of the air parcel increases, leading to even greater temperature differences from the environment, and a greater downward buoyancy force. Neither scenario provide the parcel with any CAPE.

Figure 5 shows a somewhat successful attempt to reproduce the provided parcel through back-engineering methods. In the simulation, the model parcel to follow the provided saturated adiabat, our model required e'_s to approximately quadruple e_s, indicating that the parcel was ~ 20 degrees warmer than the environment, which physically improbable. The general shape of the provided parcel temperature profile was given by Γ_d below the LCL, Γ monotonically increasing on the interval [2,6.5] $\frac{K}{Km}$ between the LCL and the LNB and $\Gamma = 3\ \frac{K}{Km}$ above the LNB.

The values of lapse rate are given below the LCL, at the LCL (the start of the saturated adiabat), at the LNB (the end of the saturated adiabat), and above the LNB are given in Table 1 for cross-model comparison. In addition to the reproduction in Figure 5, we calculated Γ of the provided parcel with the same linear least-squares fit method used to determine Γ_{env}. The provided parcel lapse rates were nonlinear on the saturated adiabat so fits were performed on 20 point intervals centered at the LCL and the LNB.

Several assumptions in our model may cause it to behave differently from an actual air parcel. For one, we assume that the air parcel in our model moves isentropically and reversibly. In reality, several processes in air parcels are not isentropic or reversible, including the process of precipitation. By not allowing any form of precipitation in our model, we greatly restricted the behavior of our air parcel. We also made several simplifying assumptions in deriving equations for lapse rates in the models. First and foremost, the environmental sounding was given without altitude measurements, and z had to be fabricated assuming a constant lapse rate on three intervals. To derive Γ_d, we assumed that the air parcel was an ideal gas. We also assumed that the parcel followed a dry adiabat until it reached 100% relative humidity. In reality, a moist adiabat would likely have a slightly smaller lapse rate than one that was completely dry. We also made several assumptions in deriving Γ_s, which were detailed in the methods section. Although our model uses this simpler expression for $d\eta$, Γ_s values determined from these assumptions are only 0.5% off of more rigorous expressions for Γ_s, suggesting that these assumptions don't appreciably hinder the model [2].

In our second model, which allows for entrainment, the entrained air is assumed to be completely dry ($w_v = 0$). In reality, the parcel would be entraining air from its surroundings, which in most cases have a much lower water vapor mixing ratio, but will not be completely dry [3]. If our model entrained air from its surroundings, rather than dry air, the air parcel lapse rate would approach that of the environment. However, this change in the model would still not allow for the air parcel temperature to be greater than the surroundings, but instead get closer to it. Entraining air that had a greater water vapor mixing ratio than the air parcel itself would allow for the magnitude of its lapse rate to decrease and behave more similarly to the provided parcel, but this process has no basis in the reality of the system. In addition, our model assumes a constant entrainment rate, but in reality the entrainment rate is dependent on a variety of factors including cloud type, temperature of the parcel and surrounding environment, and CAPE [1].

IV. CONCLUSION

We find that the simplified governing equations of adiabatic parcel rise fail to reproduce the temperature profile of the provided air parcel. Though the general shape of the parcel was reproduced in this study, physical grounds for the lapse rate values must be determined.

For future work, we would like to compare the sounding provided in Figure 7.2 to one from a database such as the University of Wyoming College of Engineering (http://weather.uwyo.edu/upperair/sounding.html). Using these parameters, we would hope to model parcel behavior as we did in this study to see if it may be possible to observe CAPE in the system. This work would be valuable in gaining insight into realistic atmospheric parameters that allow for adiabatic parcel rise and cloud formation .

[1] Cohen, Charles. *A Quantitative Investigation of Entrainment and Detrainment in Numerically Simulated Cumulonimbus Clouds.* 2000: Journal of the Atmospheric Sciences 57.10: 1657-674.

[2] Curry, Judith A., and Webster, Peter J. *Thermodynamics of Atmospheres and Oceans* 1999: San Diego: Academic.

[3] Deardorff, J. W. *Cloud Top Entrainment Instability.* 1980: Journal of the Atmospheric Sciences 37.1:131-47.

[4] Houze, Robert A. *Cloud Dynamics.* 1993: San Diego: Academic.

[5] Lu et al. *A New Approach for Estimating Entrainment Rate in Cumulus Clouds.* 2012: Geophys. Rev. Lett. 39.4.

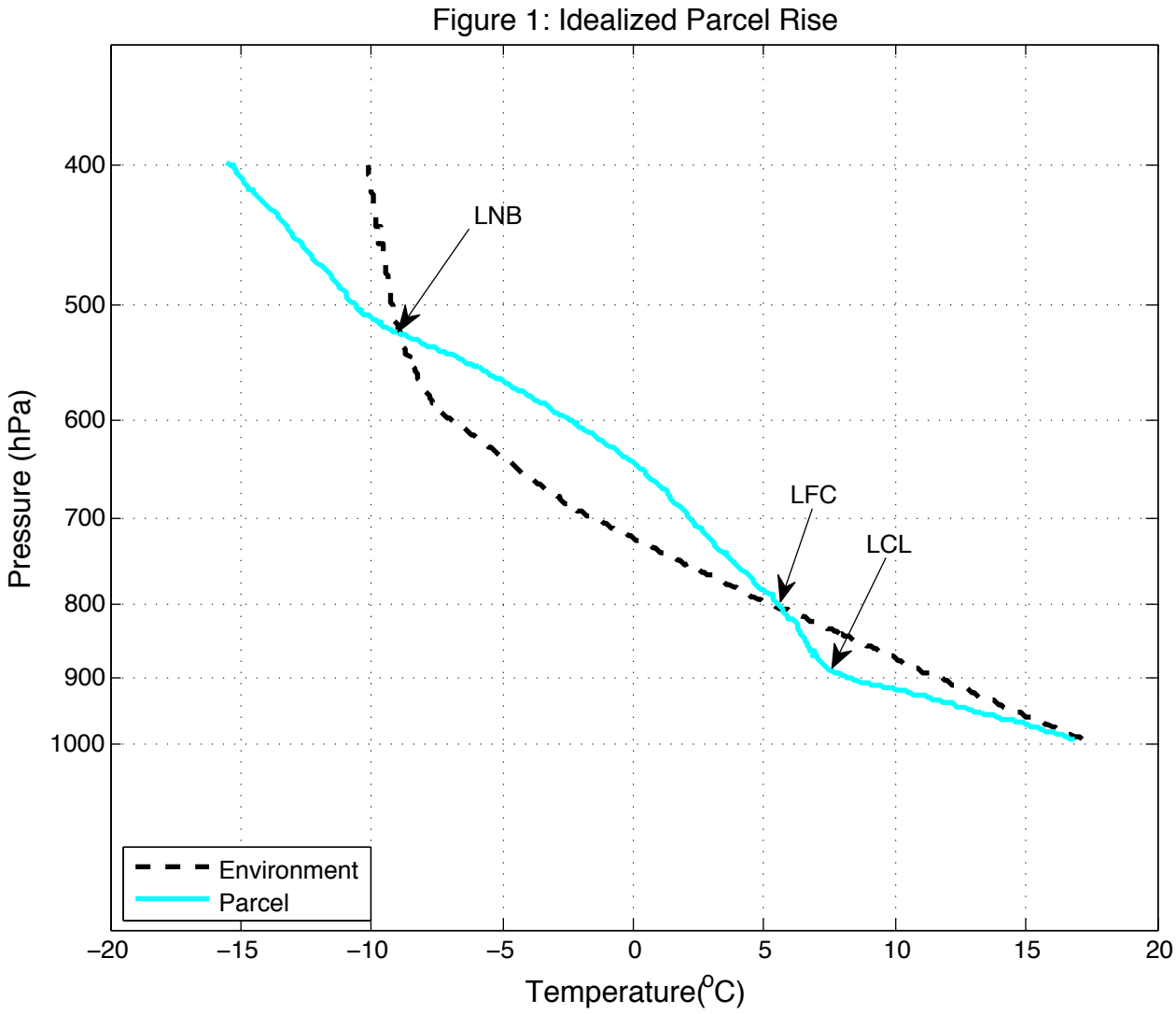

FIG. 1. The provided parcel and environmental sounding is obtained from Curry and Webster Figure 7.2 using the program Data Thief to extract data points from the graph.

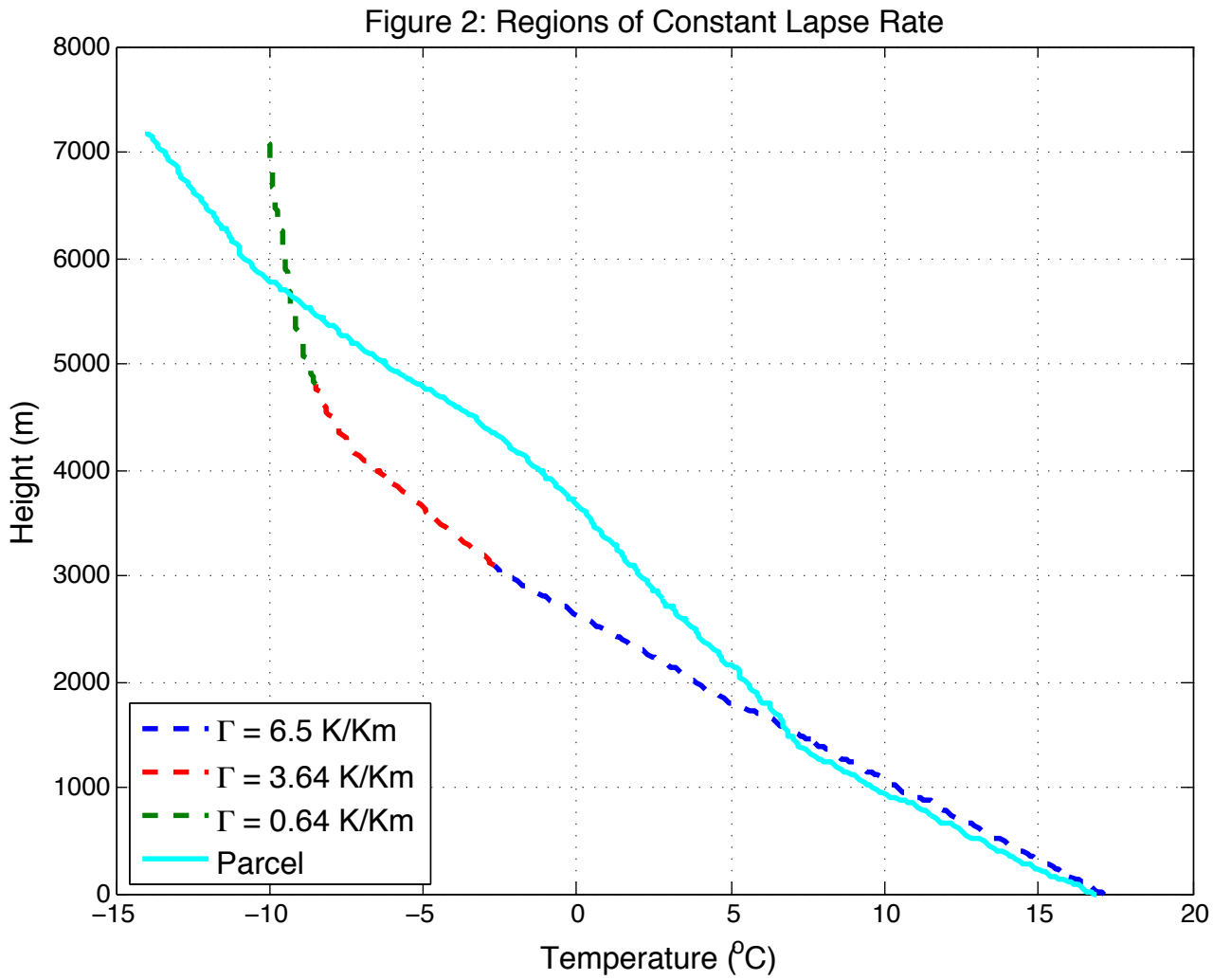

FIG. 2. Environmental lapse rates (Γ_{env}) were determined for three regions using a linear least-squares fit to the environmental sounding. Using the hypsometric equation for a constant lapse rate atmosphere in each region, we derived altitude (Z) of each sounding measurement of temperature and pressure.

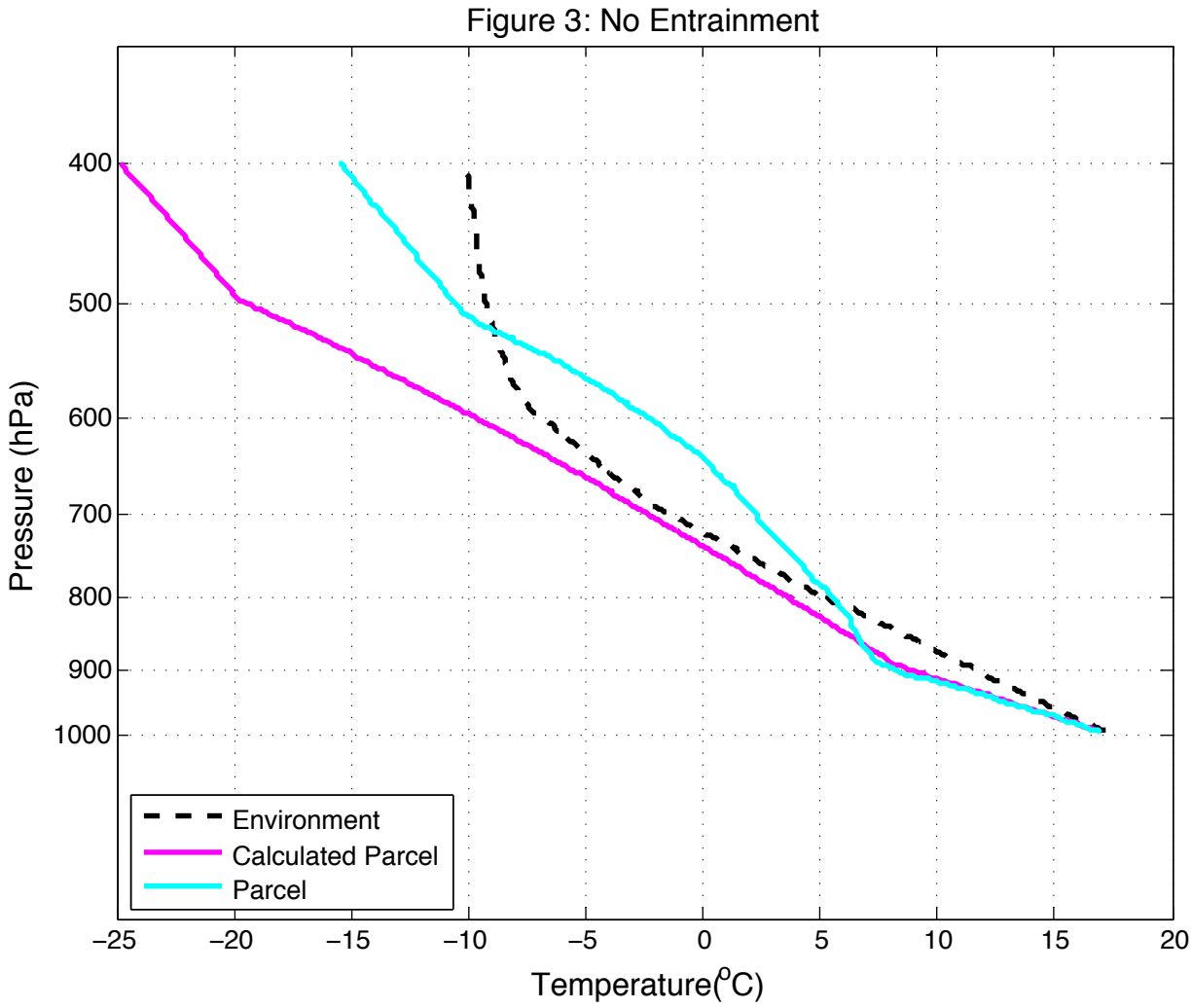

FIG. 3. Adiabatic parcel rise with no entrainment. The calculated parcel does not have the CAPE (convective available potential energy) required for adiabatic rise in the provided environment.

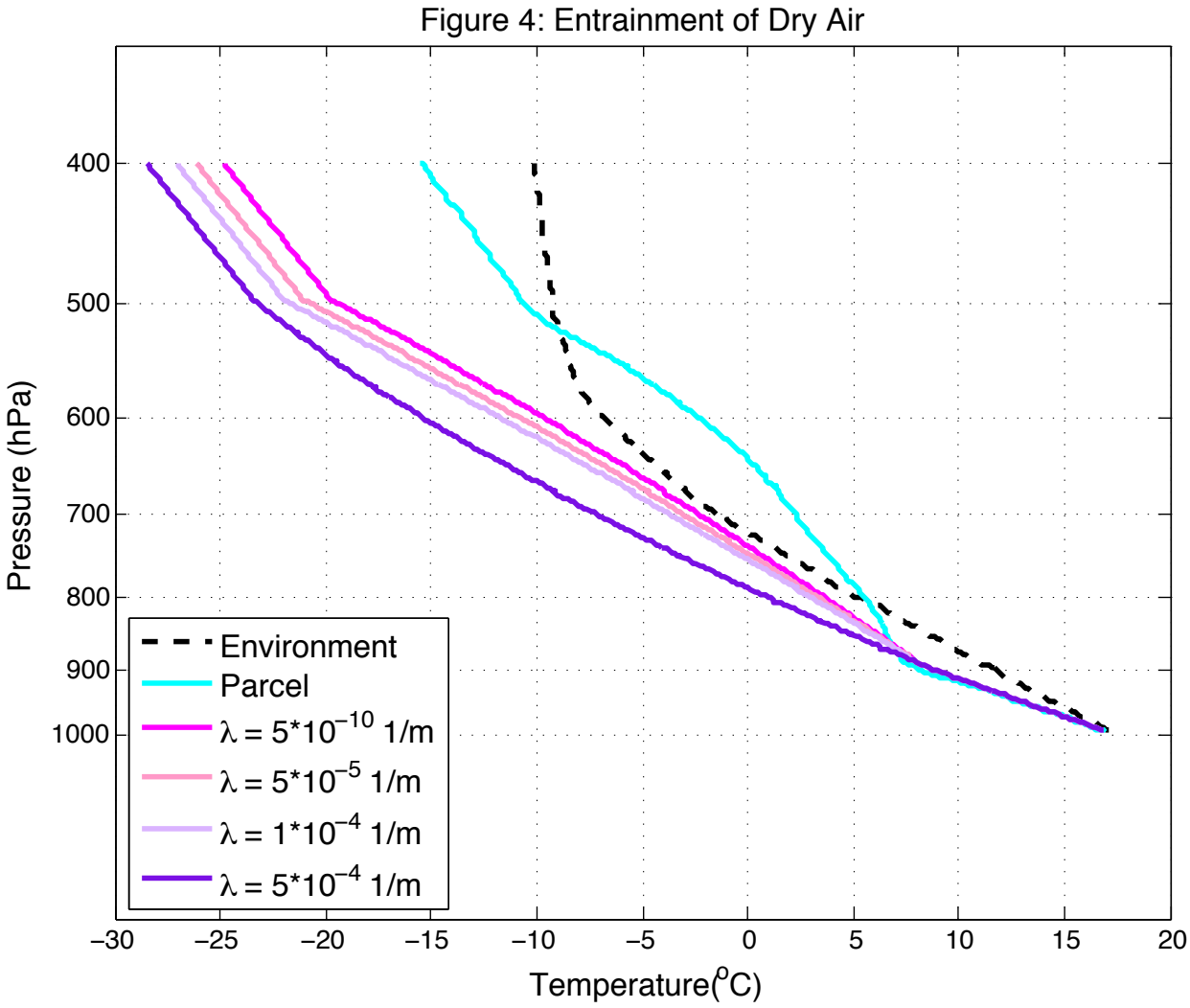

FIG. 4. Adiabatic parcel rise with entrainment of dry air. The behavior of the saturated parcel approaches that of dry adiabatic rise as more dry air is entrained.

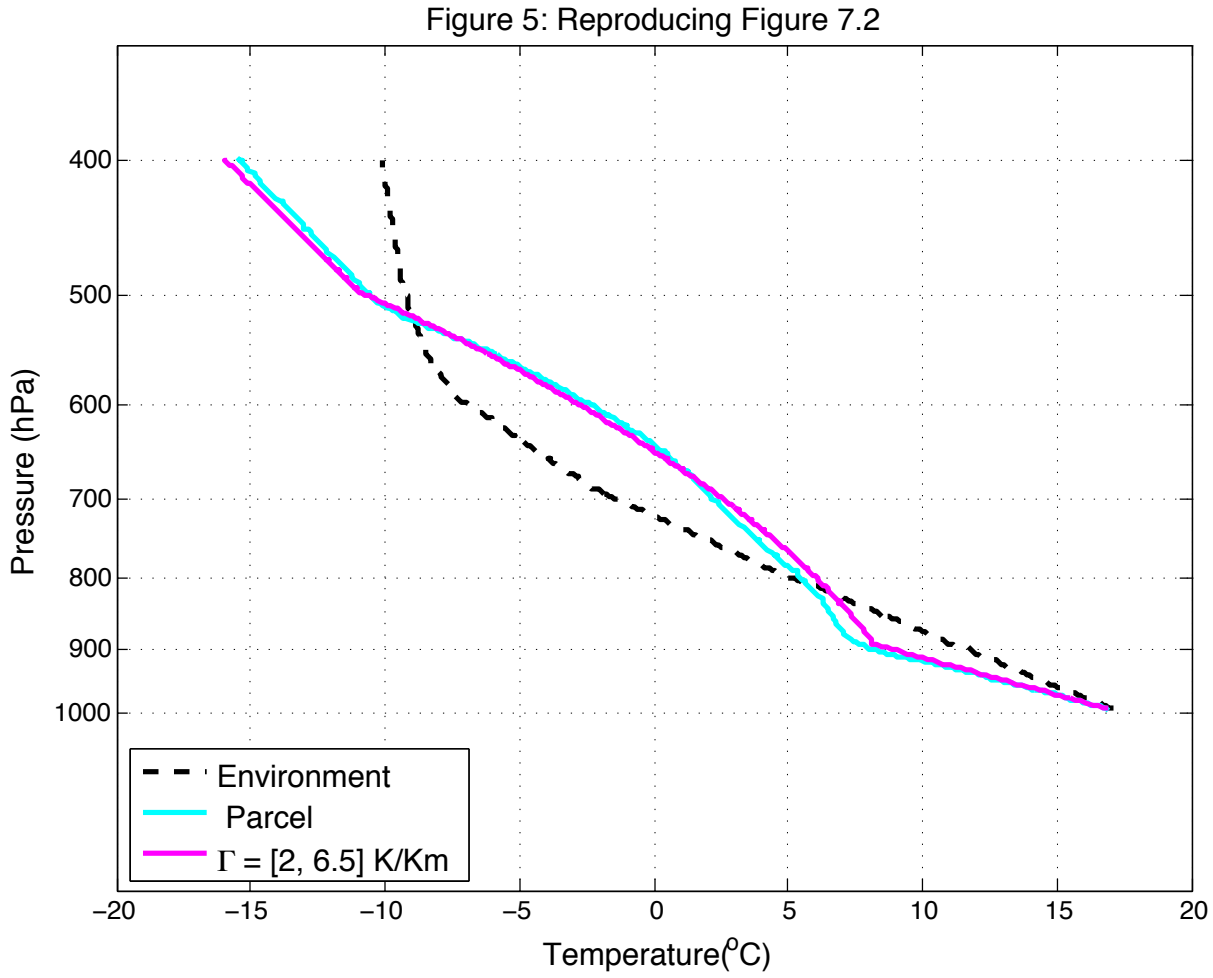

FIG. 5. While we were unable to reproduce Figure 7.2 using simplified adiabatic parcel rise, we present a reproduction after extensive sensitivity analysis. The shape of the provided saturated adiabatic rise is well reproduced by a lapse rate that monotonically increasing from $\Gamma = 2$ K/Km to $\Gamma = 6.5$ K/Km. Due the the numerous parameters governing Γ_m, we are unable to attribute its increase with height to any one parameter at this time.

	Environment	No Entrainment	λ = 5*10^-10 1/m	λ = 5*10^-5 1/m	λ = 1*10^-4 1/m	λ = 5*10^-4 1/m	Best Reproduction	Approximate Parcel
Γ to LCL	6.5	9.8	9.8	9.8	9.8	9.8	9.8	10.9
Γ at LCL	6.5	5.0	5.0	5.4	5.7	8.6	2.0	3.1
Γ at LNB	0.64	7.5	7.5	7.4	7.2	4.8	6.5	6.1
Γ above LNB	0.64	3.0	3.0	3.0	3.0	3.0	3.0	3.1

FIG. 6. The values of lapse rate are given below the LCL, at the LCL (the start of the saturated adiabat), at the LNB (the end of the saturated adiabat), and above the LNB are given in Table 1 for cross-model comparison.